

Pure 2D Visual Servo control for a class of under-actuated dynamic systems ¹

T. Hamel[†] and R. Mahony[‡]

[†]I3S, UNSA-CNRS,
2000 route des Lucioles-Les algorithmes,
06903 Sophia Antipolis, France.

[‡] Dep. of Eng.,
Australian Nat. Univ.,
ACT, 0200 Australia.

Abstract—*A pure image-based strategy for visual servo control of a class of dynamic systems is proposed. The proposed design concerns the dynamics of unmanned aerial vehicles capable of quasi-stationary flight (hover and near hover flight). The visual servo control task considered is to locate the camera relative to a stationary target. The paper extends earlier work, [6], by weakening the assumption on the construction of the visual error used. In prior work some inertial information was used in the error construction to guarantee the passivity properties of the control design. In this paper the visual error is defined purely in terms of the 2D image features derived from the camera signal.*

1 Introduction

Visual servo control concerns the problem of using a camera to provide sensor information to servo-position a robotic system. Classical visual servo control was developed for serial-link robotic manipulators with the camera typically mounted on the end-effector [7]. More recently applications involving mobile systems have been considered [11]. Visual sensing will be a vital technology for the host of low cost unmanned aerial vehicle (UAV) applications that are already under development [4, 13, 6]. Visual servo systems may be divided into two main categories [7]: 3D (*Position-Based* - involving reconstruction or pose estimation) and 2D (*Image-Based* - working directly in the image data). The first approach is a dual estimation and control problem in which the state (camera pose) of the system is estimated using visual information and the control design is a classical state-space design [7]. In the second category, the robotic task is posed directly in terms of image features rather than in Cartesian space. A controller is designed to manoeuvre the image features towards a goal configuration that implicitly solves the original Cartesian motion planning problem [12, 2, 7].

Classical *Image-Based* control design uses a simple linearising control on the image kinematics [2] that leads to complex non-linear dynamics and is not easily extended to dynamic system models. Most exist-

ing applications exploit a high gain or feedback linearisation (computed torque) design to reduce the system to a controllable kinematic model, for which the *Image-Based* visual servo techniques were developed [7]. There are very few integrated IBVS control designs for fully dynamic system models and even fewer that deal with under-actuated dynamic models. In prior work by the authors [6] proposes an IBVS control scheme for stabilization of a class of under-actuated dynamic systems that model certain types of UAV. In order to extend the control design to the full dynamic system we exploited the fundamental passivity properties of the rigid-body motion of the UAV airframe to avoid cross coupling of dynamic states in the second and third order derivatives of the image kinematics. Working within this framework it was possible to apply backstepping control design techniques and derive a control Lyapunov function for the system. Unfortunately, in order to guarantee the passivity properties of the error dynamics it was necessary to use some inertial information in the error definition and this clearly limits the applicability of the earlier work.

In this paper we study the question of using a pure image based visual error and achieving IBVS control of a class of dynamic systems associated with UAV systems capable of quasi-stationary flight. The visual feature considered is a simple weighted centroid feature and the goal feature is fixed in the camera image. To understand the difficulty of the associated control problem, imagine a UAV (such as a helicopter) hovering above a fixed target. Imagine that the observed target is slightly to the left of the goal vector in the image. Due to the dynamics of the vehicle, in order to move left the airframe must be inclined to the left, leading the observed landmark moving left in the image while the goal target remains fixed in the image. It follows that to design a stable IBVS control algorithm it is necessary to allow the image error to increase locally in order to allow the system dynamics to act to move the UAV to the desired position such that when the attitude of the UAV is stabilized the image error will be zero. The material presented in the present paper is an extension of our previous work [6] where inertial information was used to modify the goal target in order to avoid the situation just described. In this paper, we deal with the effects of a fixed goal target by treating

¹This research was supported in part by "Ministère de la Jeunesse, de l'Éducation Nationale et de la Recherche" of the France government and by CNRS ROBEA Grant.

them as perturbations of the first order image kinematics bounded by error terms that can be derived from the higher order dynamic stabilization problem. In this manner we propose a decoupled control design followed by a fully coupled stability and robustness analysis of the system using a structured control Lyapunov function construction. Since the image error construction relies purely on information derived from the 2D image data we refer to the approach as pure 2D visual servo control. It is still necessary estimate and compensate for the direction and magnitude of gravity using an inertial measurement unit that also provides velocity measurements.

The paper is organised as follows: Section 2 presents the dynamic system model considered. Section 3 describes the visual features and defines the image based error used. Section 4 derives a Lyapunov control function for the positioning task and analysis the stability of the closed-loop system. Section 5 applies the control strategy to a simplified model for the dynamics of a four rotor vertical take-off and landing (VTOL) vehicle known as an X4-flyer [5, 1] and presents some simulation results. The final section provides a short summary of conclusions.

2 Problem Formulation.

In this section, we present the fundamental equations of motion of unmanned aerial vehicles capable of stationary hovering at one location. The system model considered in the sequel is equivalent to those introduced in the literature to model the dynamics of helicopters [13, 3]. Let $\mathcal{I} = \{E_x, E_y, E_z\}$ denote the world frame and let $\mathcal{A} = \{E_1^a, E_2^a, E_3^a\}$ denote the body-fixed frame of the rigid body. The position of the rigid body in the world frame is denoted $\xi = (x, y, z) \in \mathcal{I}$ and its attitude (or orientation) is given by a rotation $R: \mathcal{A} \rightarrow \mathcal{I}$, where $R \in SO(3)$ is an orthogonal rotation matrix. Let V (resp. Ω) denote the linear (resp. angular) velocity of the body expressed in the body fixed frame. Let m denote the total mass and $\mathbf{I} = \text{diag}(\mathbf{I}_1, \mathbf{I}_2, \mathbf{I}_3)$ a diagonal matrix denoting the inertia of the body. The dynamics of a rigid body are¹:

$$\dot{\xi} = RV \quad (1)$$

$$m\dot{V} = -m\Omega \times V + F = -\text{msk}(\Omega)V + F \quad (2)$$

$$\dot{R} = R\text{sk}(\Omega), \quad (3)$$

$$\mathbf{I}\dot{\Omega} = -\Omega \times \mathbf{I}\Omega + \Gamma = -\text{sk}(\Omega)\mathbf{I}\Omega + \Gamma. \quad (4)$$

The exogenous force and torque are denoted F and Γ respectively (cf. Fig. 1) The exogenous force and torque inputs considered correspond to a typical arrangement found on a VTOL aircraft (cf. Sec. 5). The exogenous inputs are written as a single translational force, denoted F in Figure 1, along with full torque control,

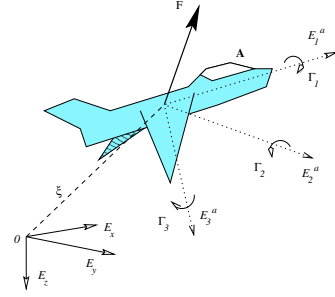


Figure 1: Reference frames, forces and torques for an Unmanned Aerial Vehicle (UAV).

shown by the torques Γ_1 , Γ_2 and Γ_3 around axes E_1^a , E_2^a and E_3^a respectively. The force F combines thrust, lift, gravity and drag components. It is convenient to separate the gravity component $mgE_z = mgR^T e_3$ from the thrust force²

$$F := -Te_3 + mgR^T e_3 \quad (5)$$

where $T \in \mathbb{R}$ is a scalar input representing the magnitude of external force applied in direction e_3 . Control of the airframe is obtained by using the torque control $\Gamma = (\Gamma_1, \Gamma_2, \Gamma_3)$ to align the force $F_0 := Te_3$ as required to track the goal trajectory.

3 Image Dynamics

In visual servo control problems, the image dynamics must be expressed in the frame of reference of the camera. Since we consider ‘eye-in-hand’ configurations, the motion of the camera frame inherits dynamics in the body fixed frame. In order to simplify the derivation in the sequel, it is assumed that the camera fixed frame coincides with the body fixed frame \mathcal{A} . Let a set of n points P'_i of a fixed target ($\dot{P}'_i = 0$), relative to the inertial frame (\mathcal{I}) and observed from the camera, and let P_i be the representation of P'_i in the camera fixed frame, then P_i is given by

$$P_i = R^T(P'_i - \xi)$$

A backstepping control design has passivity-like properties from virtual input to the backstepping error [8]. In our previous work [6] it was shown that these structural passivity-like properties are present in the image space dynamics *if and only if* the spherical projection of an observed point is used. Denoting the spherical projection of an image point P_i by p_i the image dynamics are given by:

$$\dot{p}_i = -\text{sk}(\Omega)p_i + \pi_p \frac{V}{r_i} \quad (6)$$

¹The notation $\text{sk}(\Omega)$ denotes the skew-symmetric matrix such that $\text{sk}(\Omega)v = \Omega \times v$ for the vector cross-product \times and any vector $v \in \mathbb{R}^3$.

²This is a reasonable approach for the dynamics of a UAV in quasi-stationary flight. The implication of this decomposition is the key of our control strategy (Sec. 4).

Here $r_i = |P_i|$ (the focal length is assumed to be unity for simplicity). The matrix $\pi_p = (I - p_i p_i^T)$ is the projection onto the tangent space of the spherical image surface at the point p_i (I is the 3×3 identity matrix).

For a given target the centroid of the target based on spherical information is defined to be

$$q := \sum_{i=1}^n p_i \in \mathbb{R}^3 \quad (7)$$

As defined in [6], the above centroid contains more information than the classical image blob centroid. Here the norm of the image feature $|q|$ encodes effective depth information. When the target points are far from the camera all the $\{p_i\}$ are co-linear and the norm is maximal. As the camera moves toward the target points they spread in the image and cancel each other in the summation leading to a decrease in the norm $|q|$. Thus, the image feature q contains three effective degrees of information and can be used as the basis of a position stabilization control design.

Recalling Eq. 6, it may be verified that

$$\dot{q} = -\Omega \times q - QV, \quad (8)$$

where

$$Q = \sum_{i=1}^{i=n} \frac{\pi p_i}{r_i} > 0. \quad (9)$$

The visual servo control task considered is that of positioning a camera relative to a stationary (in the inertial frame) target. In our previous work [6], in addition to visual information additional inertial information is explicitly used in the error formulation. In particular, the inertial direction of the goal target in the image is fixed. That is a goal q^* was chosen that has fixed inertial orientation and moves in the image plane. The advantage of such a choice is clear when one recalls the example mentioned in the introduction of a UAV (such as a helicopter) hovering above a fixed target. If the image vector has fixed inertial direction, then as the UAV tilts the image error does not change. The goal vector $q^*(t)$ moves in the (spherical) image plane in exactly the same manner as the observed target. It is only as the vehicles changes its position that the image error changes. In prior work [6], this property was exploited to decouple the position stabilization from the attitude stabilization problem. If no inertial information for the goal vector is known then it is necessary to define a fixed goal vector and deal with coupled dynamic equations.

Define $q^* \in \mathcal{A}$ to be the desired target vector expressed in the camera fixed frame.

$$q^* := (q_1^*, q_2^*, q_3^*)^T \in \mathcal{A}$$

The norm $|q^*|$ encodes the effective depth information for the desired limit point while the direction of q^* defines the camera attitude up to rotation around the

axis q^* . It is necessary that q^* defines a goal that is attainable by the vehicle considered otherwise the dynamic model of the vehicle will not be in equilibrium when $q = q^*$.

The image based error considered is the difference between the measured centroid and the target vector expressed in the camera fixed frame

$$\delta_1 := q - q^*. \quad (10)$$

Deriving δ_1 yields:

$$\dot{\delta}_1 = -\text{sk}(\Omega)\delta_1 - QV - \text{sk}(\Omega)q^* \quad (11)$$

The above equation (Eq. 11) defines the kinematics of the visual error δ_1 .

It is of interest to study the structural properties of Eq. 11. Consider the storage function $|\delta_1|^2$. The derivative of this function is

$$\frac{d}{dt}|\delta_1|^2 = -\delta_1^T \text{sk}(\Omega)\delta_1 - \delta_1^T QV - \delta_1^T \text{sk}(\Omega)q^*.$$

The first term is zero due to the skew symmetry of Ω . Since the matrix $Q > 0$ is positive definite, the second term can be seen as an inner product between δ_1 and V . In this sense we think of the second term as a the supply function to the storage function. Choosing $V = \delta_1$ acts to decrease $|\delta_1|^2$. The last term is the perturbation due to the fixed goal assumption and was not present in the prior work of the authors [6] due to the choice of an inertial goal vector. When the goal vector is fixed in the image plane it is impossible to avoid the presence of the perturbation term. The term resembles the perturbations due to small-body forces that lead to zero dynamic effects studied in recent works [4, 9]. This sort of term is particularly difficult to deal with explicitly in the control design. It depends on the angular velocity Ω and destroys the triangular nature of the system that is necessary to apply the backstepping approach. The approach taken in this paper is to leave this term as a perturbation of the stability analysis of the first order image kinematics. By choosing the control gains governing the higher order backstepping errors correctly this error perturbation can be controlled and dominated in the integrated stability analysis.

The image Jacobian³ [7] (denoted J) is obtained by rewriting Eq. 11 in the classical form

$$\dot{\delta}_1 = \begin{bmatrix} Q & \text{sk}(q^*) + \text{sk}(\delta_1) \end{bmatrix} \begin{pmatrix} V \\ \Omega \end{pmatrix} = J \begin{pmatrix} V \\ \Omega \end{pmatrix}.$$

In common with classical IBVS algorithms, the image Jacobian depends on the unknown depth of the image features. That is, although the points $\{p_i\}$ are known, the depth parameters $\{|P_i|\}$ cannot be measured directly from visual data. However, for the proposed image error the unknown parameters enter only into the

³Also known as the interaction matrix [2].

definition of the matrix Q (Eq. 9), and here they enter in a structured manner such that the matrix $Q > 0$ is always positive definite. It is this property that is exploited in Section 4 in the control design, avoiding the necessity of estimating or approximating the image Jacobian, a fundamental difficulty in most IBVS algorithms [2, 7, 10]. In the present development we consider a region in space on which the matrix Q is uniformly bounded

$$\lambda_{\min} < \{\lambda_i(Q)\} < \lambda_{\max} \quad (12)$$

by two arbitrary bounds, $\lambda_{\max} > \lambda_{\min} > 0$, and design a robust control algorithm valid on the entire region considered.

4 Visual servo control for a VTOL aircraft

In this section, a control design based on robust backstepping techniques [8] is proposed for visual servo control of the under-actuated system that we consider. The full dynamics of the error δ_1 may be written:

$$\dot{\delta}_1 = -\text{sk}(\Omega)\delta_1 - QV - \text{sk}(\Omega)q^* \quad (13)$$

$$m\dot{V} = -m\Omega \times V + F = -\text{msk}(\Omega)V + F \quad (14)$$

$$\dot{R} = R\text{sk}(\Omega), \quad (15)$$

$$\mathbf{I}\dot{\Omega} = -\Omega \times \mathbf{I}\Omega + \Gamma = -\text{sk}(\Omega)\mathbf{I}\Omega + \Gamma. \quad (16)$$

Before introducing the main result of the paper, we introduce the following change of variables:

$$\delta_2 = \frac{m}{k_1}V - \delta_1, \quad (17)$$

$$\delta_3 = \frac{m}{k_1^2 k_2} (-Te_3 + mgR^T e_3) + \delta_2 \quad (18)$$

The error δ_2 is introduced to regulate the linear velocity of the camera and ensures that it comes to rest. The additional error vector δ_3 incorporates information on the attitude of the camera. This is natural for a system such a VTOL aircraft capable to do stationary flight since the desired motion can only be obtained by exploiting the attitude dynamics to regulate δ_1 . If the position and linear velocity are regulated then the total external force must be zero, $-Te_3 + mgR^T e_3 = 0$. It follows then,

$$Re_3 = e_3, \quad T = mg. \quad (19)$$

This means that the pitch and roll rotations of the rigid body are directly stabilised via the stabilisation of the error δ_3 . However, the yaw rotation around the direction e_3 is not concerned by the stabilisation of the error δ_3 . To stabilize this remaining degree of freedom an additional error criteria independent of q must be used [6]. In this paper and in order to simplify the analysis in the sequel, a simple proportional control is used to stabilise the yaw angular velocity. More precisely, we apply a linearising control in the third component

of angular velocity to set, $\Omega_3(0) = 0$ and apply a stabilizing control to add robustness to the design

$$\Gamma_3 = e_3^T (\Omega \times \mathbf{I}\Omega) - k_\Omega \Omega_3 \quad (20)$$

where k_Ω is a suitable gain. The proposed control algorithm, in the sequel, requires a formal time derivative of the input T [6]. To provide this input, T is dynamically extended.

$$\dot{T} = U \quad (21)$$

The motivation for adding an integrator is to ensure decoupling between translational and rotational dynamics as shown in the sequel.

Recalling Eqn's 13-25, the full dynamics of the visual error δ_1 in terms of the additional errors δ_i ($i = 1 \dots 3$) can be written:

$$\dot{\delta}_1 = -\text{sk}(\Omega)\delta_1 - \frac{k_1}{m}Q\delta_1 - \frac{k_1}{m}Q\delta_2 + \text{sk}(q^*)\Omega \quad (22)$$

$$\begin{aligned} \dot{\delta}_2 = & -\text{sk}(\Omega)\delta_2 + \frac{k_1}{m}Q\delta_1 - \frac{k_1}{m}(k_2 I - Q)\delta_2 + \frac{k_1 k_2}{m}\delta_3 \\ & - \text{sk}(q^*)\Omega \end{aligned} \quad (23)$$

$$\begin{aligned} \dot{\delta}_3 = & -\text{sk}(\Omega)\delta_3 + \frac{k_1}{m}Q\delta_1 - \frac{k_1}{m}(k_2 I - Q)\delta_2 + \frac{k_1 k_2}{m}\delta_3 \\ & + \frac{m}{k_1^2 k_2} \left(\text{sk} \left(Te_3 - \frac{k_1^2 k_2}{m} q^* \right) \Omega - \dot{T} e_3 \right) \end{aligned} \quad (24)$$

Define δ_4 as a last error term. It is introduced to regulate the pitch and roll angular velocities as

$$\delta_4 = \frac{m^2}{k_1^2 k_2 (k_1 k_2 + k_3)} \pi_{e_3} \text{sk} \left(Te_3 - \frac{k_1^2 k_2}{m} q^* \right) \Omega + \pi_{e_3} \delta_3, \quad (25)$$

where $\pi_{e_3} = (I - e_3 e_3^T)$.

Introducing Eqn's 21 and 25 in the expression of the derivative of error δ_3 (Eq. 24), it yields

$$\begin{aligned} \dot{\delta}_3 = & -\text{sk}(\Omega)\delta_3 + \frac{k_1}{m}Q\delta_1 - \frac{k_1}{m}(k_2 I - Q)\delta_2 + \frac{k_1 k_2 + k_3}{m} \pi_{e_3} \delta_4 \\ & - \frac{k_3}{m} \delta_3 - (I - \pi_{e_3}) \left(\text{sk}(q^*)\Omega - \frac{k_1 k_2 + k_3}{m} \delta_3 + \frac{m}{k_1^2 k_2} U e_3 \right) \end{aligned} \quad (26)$$

Deriving the expression of δ_4 (Eq. 25) and recalling Eqn's 22, 23, 21 and 26, it yields

$$\begin{aligned} \dot{\delta}_4 = & -\pi_{e_3} \text{sk}(\Omega)\delta_3 + \frac{k_1}{m} \pi_{e_3} Q\delta_1 - \frac{k_1}{m} \pi_{e_3} (k_2 I - Q)\delta_2 \\ & + \frac{k_1 k_2 + k_3}{m} \pi_{e_3} \delta_4 + \frac{m^2}{k_1^2 k_2 (k_1 k_2 + k_3)} \pi_{e_3} U \text{sk}(e_3) \Omega \\ & - \frac{k_3}{m} \pi_{e_3} \delta_3 + \frac{m^2}{k_1^2 k_2 (k_1 k_2 + k_3)} \pi_{e_3} \text{sk} \left(Te_3 - \frac{k_1^2 k_2}{m} q^* \right) \dot{\Omega} \end{aligned} \quad (27)$$

Using the previous assumption ($\Omega_3 = 0, \forall t \in R^+$) and considering only the existence of roll and pitch velocities, the expressions of the derivatives of the errors δ_3

and δ_4 become:

$$\begin{aligned} \dot{\delta}_3 = & -\text{sk}(\Omega)\delta_3 + \frac{k_1}{m}Q\delta_1 - \frac{k_1}{m}(k_2I - Q)\delta_2 + \frac{k_1k_2 + k_3}{m}\pi_{e_3}\delta_4 \\ & - \frac{k_3}{m}\delta_3 - (I - \pi_{e_3}) \left(\text{sk}(q^*)\pi_{e_3}\Omega - \frac{k_1k_2 + k_3}{m}\delta_3 + \frac{m}{k_1^2k_2}Ue_3 \right) \end{aligned} \quad (28)$$

$$\begin{aligned} \dot{\delta}_4 = & -\pi_{e_3}\text{sk}(\Omega)\delta_3 + \frac{k_1}{m}\pi_{e_3}Q\delta_1 - \frac{k_1}{m}\pi_{e_3}(k_2I - Q)\delta_2 \\ & + \frac{k_1k_2 + k_3}{m}\pi_{e_3}\delta_4 + \frac{m^2}{k_1^2k_2(k_1k_2 + k_3)}\pi_{e_3}U\text{sk}(e_3)\pi_{e_3}\Omega \\ & - \frac{k_3}{m}\pi_{e_3}\delta_3 + \frac{m^2}{k_1^2k_2(k_1k_2 + k_3)}\pi_{e_3}\text{sk} \left(Te_3 - \frac{k_1^2k_2}{m}q^* \right) \pi_{e_3}\dot{\delta}_3 \end{aligned} \quad (29)$$

It is now possible to present the main result of the paper:

Theorem 4.1 *Consider the dynamics given by Eqn's 22-29. Let λ_{\max} be the maximal bound on eigenvalues of Q . Let the vector controller given by :*

$$U = \frac{k_1^2k_2}{m} \frac{k_1k_2 + k_3}{m} e_3^T \delta_3 - \frac{k_1^2k_2}{m} e_3^T \text{sk}(q^*)\Omega \quad (30)$$

$$\begin{aligned} \Gamma = \mathbf{I}^{-1} \left(\text{sk}(\Omega)\mathbf{I}\Omega - k_\Omega\Omega_3e_3 - \frac{\mathbf{I}}{T - \frac{k_1^2k_2}{m}q_3^*} U\text{sk}(e_3)\Omega \right. \\ \left. - \frac{k_1^2k_2(k_1k_2 + k_3)}{m^2}\text{sk}(e_3) \left(\text{sk}(\Omega)\delta_3 + \frac{k_1k_2}{m}\delta_2 - \frac{k_1k_2}{m}\delta_3 \right. \right. \\ \left. \left. - \frac{k_1k_2 + k_3 + k_4}{m}\delta_4 \right) \right) \end{aligned} \quad (31)$$

Let \mathcal{L} be the Lyapunov function candidate:

$$\mathcal{L} = \frac{1}{2}|\delta_1|^2 + \frac{1}{2}|\delta_2|^2 + \frac{1}{2}|\delta_3|^2 + \frac{1}{2}|\delta_4|^2 \quad (32)$$

Set

$$f(T) = \frac{k_1k_2(k_1k_2 + k_3)}{m \left(T - \frac{k_1^2k_2}{m}q_3^* \right)}$$

and choose the positive control gains to satisfy

$$\begin{aligned} k_2 &> \lambda_{\max}, \\ k_1 &< \sqrt{\frac{2mgq_3^*}{k_2}}, \\ k_3 &> \frac{(k_2 + \lambda_{\max})(\lambda_{\max} + f(T_{\min})|q^*|)^2}{\lambda_{\min}(k_2 - \lambda_{\max})}, \quad T_{\min} = 2\frac{k_1^2k_2}{m}q_3^* \\ k_4 &> 0. \end{aligned}$$

Then, for any initial condition such that the initial value of the Lyapunov function candidate

$$\begin{aligned} \mathcal{L}(0) = & \frac{1}{2}|\delta_1(0)|^2 + \frac{1}{2}|\delta_2(0)|^2 \\ & + \frac{1}{2}|\delta_3(0)|^2 + \frac{1}{2}|\delta_4(0)|^2 < \frac{1}{2} \left(\frac{mg}{k_1^2k_2} - 2q_3^* \right)^2, \end{aligned} \quad (33)$$

the Lyapunov function is exponentially decreasing, ensuring exponential stability of the errors δ_i for $i = 1..4$.

Proof: Recall that:

$$\dot{\Omega} = -\mathbf{I}^{-1}\text{sk}(\Omega)\mathbf{I}\Omega + \mathbf{I}^{-1}\Gamma$$

using the fact that:

$$\pi_{e_3}\text{sk} \left(Te_3 - \frac{k_1^2k_2}{m}q^* \right) \pi_{e_3} = \left(T - \frac{k_1^2k_2}{m}q_3^* \right) \text{sk}(e_3)$$

and that $\pi_{e_3}\delta_4 = \delta_4$,

taking the derivative of \mathcal{L} (substituting from Eqn's 22-23, 28-29 and using the feedback control given by Eqn's 30 and 31) it yields:

$$\begin{aligned} \dot{\mathcal{L}} = & -\frac{k_1}{m}\delta_1^T Q\delta_1 - \frac{k_1}{m}\delta_2^T (k_2I_3 - Q)\delta_2 - \frac{k_3}{m}|\delta_3|^2 - \frac{k_4}{m}|\delta_4|^2 \\ & + \frac{k_1}{m}\delta_3^T Q\delta_1 + \frac{k_1}{m}\delta_3^T Q\delta_2 + \frac{k_1}{m}\delta_4^T Q\delta_1 + \frac{k_1}{m}\delta_4^T Q\delta_2 \\ & + (\delta_1 - \delta_2)^T \text{sk}(q^*)\Omega \end{aligned} \quad (34)$$

Note that, due to the presence of the vector Ω , the Lyapunov function may not be monotonically decreasing. Recalling the expression of the error term δ_4 Eq. 25, it yields:

$$\pi_{e_3}\Omega = -\frac{k_1}{m}f(T)\text{sk}(e_3)(\delta_4 - \delta_3) \quad (35)$$

Introducing now the above relationship in Eq. 34 the Lyapunov function derivative becomes:

$$\begin{aligned} \dot{\mathcal{L}} = & -\frac{k_1}{m}\delta_1^T Q\delta_1 - \frac{k_1}{m}\delta_2^T (k_2I_3 - Q)\delta_2 - \frac{k_3}{m}|\delta_3|^2 - \frac{k_4}{m}|\delta_4|^2 \\ & + \frac{k_1}{m}\delta_3^T (Q - f(T)A)\delta_1 + \frac{k_1}{m}\delta_3^T (Q + f(T)A)\delta_2 \\ & + \frac{k_1}{m}\delta_4^T (Q + f(T)A)\delta_1 + \frac{k_1}{m}\delta_4^T (Q - f(T)A)\delta_2 \end{aligned}$$

where $A = -\text{sk}(q^*)\text{sk}(e_3)$

From the above development, one has:

$$\dot{\mathcal{L}} \leq -X^T \Sigma X$$

where $X^T = [\delta_1 \ \delta_2 \ \delta_3 \ \delta_4]$ and

$$\Sigma = \begin{pmatrix} k_1Q & 0 & -\frac{k_1}{2}M & -\frac{k_1}{2}N \\ 0 & k_1(k_2I - Q) & -\frac{k_1}{2}N & -\frac{k_1}{2}M \\ -\frac{k_1}{2}M & -\frac{k_1}{2}N & k_3 & 0 \\ -\frac{k_1}{2}N & -\frac{k_1}{2}M & 0 & k_4 \end{pmatrix}$$

where:

$$\begin{aligned} M &= (Q - f(T)A^T) \\ N &= (Q + f(T)A^T) \end{aligned}$$

The above quadratic expression is negative definite if and only if the symmetric matrix Σ is positive definite. This is true if and only if the principal minors of Σ are positive. It yields then, the following sufficient conditions:

$$\begin{aligned} k_1 &> 0, \\ k_2 &> \lambda_{\max}, \\ k_3 &> \frac{(k_2 + \lambda_{\max})(\lambda_{\max} + f(T)\|AA^T\|_{\frac{1}{2}})^2}{\lambda_{\min}(k_2 - \lambda_{\max})}, \\ k_4 &> 0. \end{aligned}$$

In order to derive the conditions provided by the theorem statement, the following two sided bound on the control T are obtained from Eq. 18:

$$mg - \frac{k_1^2 k_2}{m} (|\delta_2| + |\delta_3|) < T < mg + \frac{k_1^2 k_2}{m} (|\delta_2| + |\delta_3|)$$

Combining the above two sided bound with the expression of the Lyapunov function, it follows:

$$mg - \frac{k_1^2 k_2}{m} \sqrt{2\mathcal{L}} < T < mg + \frac{k_1^2 k_2}{m} \sqrt{2\mathcal{L}}$$

From Eq. 31, the uniqueness of the control input is guaranteed as long as $T \neq \frac{k_1^2 k_2}{m} q_3^*$.

Using Eq. 33 and condition on the gain k_1 of the theorem, it yields the following bound on the initial condition of the control T :

$$2 \frac{k_1^2 k_2}{m} |q^*| < mg - \frac{k_1^2 k_2}{m} \sqrt{2\mathcal{L}_0} < T_0 < mg + \frac{k_1^2 k_2}{m} \sqrt{2\mathcal{L}_0}$$

It remains to show that this inequality is verified for $\forall t \in \mathbb{R}^+$.

By continuity, the choice of gains k_1, \dots, k_4 ensures the positiveness of the principal minors of the matrix Σ and the result is proved. ■

5 Example System and Simulation

In this section, the procedure presented in Section 4 is applied to an idealized model of the dynamics of an X4-flyer.

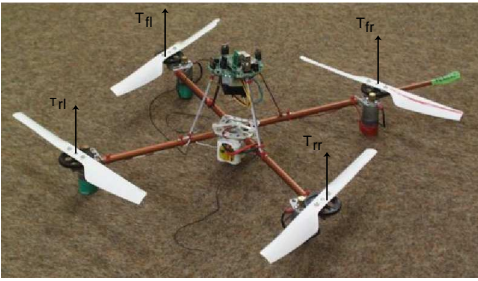


Figure 2: A prototype (un-instrumented) X4-flyer with thrust inputs.

An X4-flyer consists of four individual fans fixed to a rigid cross frame (cf. Fig. 2). It operates as an omnidirectional vehicle capable of quasi-stationary flight. An idealized dynamic model of the X4-flyer [5, 1] is given by the rigid body equations (Eqn's 1-16) along with the external force and torque inputs are (cf. Fig. 2):

$$T = T_{rr} + T_{rl} + T_{fr} + T_{fl}, \quad (36)$$

$$\Gamma_1 = d(T_{fr} + T_{fl} - T_{rr} - T_{rl}), \quad (37)$$

$$\Gamma_2 = d(T_{rl} + T_{fl} - T_{rr} - T_{fr}), \quad (38)$$

$$\Gamma_3 = \kappa (T_{fr} + T_{rl} - T_{fl} - T_{rr}). \quad (39)$$

The individual thrust of each motor is denoted $T_{(\cdot)}$, while κ is the proportional constant giving the induced couple due to air resistance for each rotor and d denotes the distance of each rotor from the centre of mass of the X-4 flyer.

The parameters used for the dynamic model are $m = 9.6$, $I = \text{diag}(0.4, 0.56, 0.22)$, $d = 0.25\text{m}$, $\kappa = 0.01$ and $g = 9.8$.

The simulation undertaken considers the case of stabilisation of the X4-flyer already in hover flight to a new set point several metres distance from the initial condition. Consider the case where one wishes to position the camera parallel to a plan target characterised by a square. In the case of a pin-hole camera the visual measurements available are the projective coordinates of the four points defining the square. These coordinates are then transformed into spherical coordinates. The desired target vector q^* is chosen such that the camera set point is located 3 metres above the square. For the simulation undertaken, the values

$$\lambda_{\min} = 0.01\text{m}^{-1} \text{ and } \lambda_{\max} = 5\text{m}^{-1}$$

were chosen. The region in task space for which these bounds remain valid is a compact set that excludes the target points (cf. Figure 3).

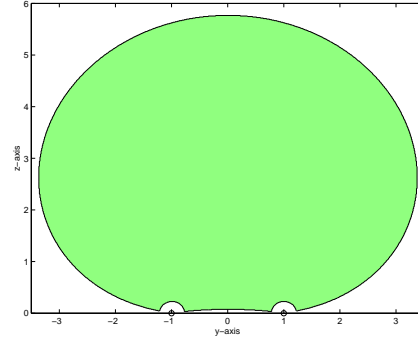


Figure 3: A cross section in the $(x(\text{or } y), z)$ plane of region for which the bounds $\lambda_{\max} < 5$, $\lambda_{\min} > 0.01$ are valid

The initial condition was chosen such that the X4 was in stable stationary flight in the specified region (Fig. 3) at the beginning of the simulation

$$\xi_0 = (5 \ 2.5 \ -4)^T, \quad R_0 = I_3, \quad \dot{\xi}_0 = \dot{\Omega} = 0.$$

According to standard aeronautical conventions height is measured down relative to the aircraft and hence the height of the X4 is negative with respect to the world frame.

According to the theorem statement, the control gains used were $k_1 = 0.2 \text{ kg.m.s}^{-1}$, $k_2 = 10 \text{ kg}^{-1}$, $k_3 = 30.5 \text{ kg.s}^{-1}$, $k_4 = 3 \text{ kg.s}^{-1}$. These gains satisfy the conditions of the theorem.

In Figures 4-5, the performances of the algorithm are shown.

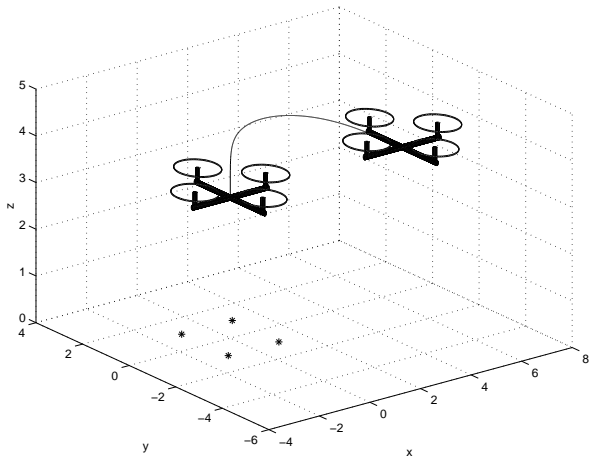


Figure 4: Positioning of the X4-flyer with respect to the target.

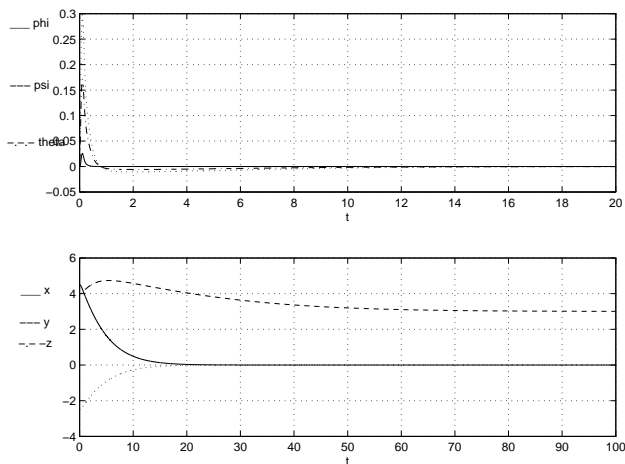


Figure 5: Evolution of the attitude and position of the X4-flyer in "roll (theta), pitch (psi) and yaw (phi)" Euler angles and Cartesian space coordinates (x , y , and z).

6 Conclusion

This paper has proposed a pure image-based strategy for visual servo control of a class of under-actuated dynamic systems. It extends our previous work [6] by avoiding the use of some inertial information in the definition of the visual error. After tedious but standard calculation, we have proposed a decoupled (position from orientation dynamics) control design followed by a fully coupled stability and robustness analysis. The simulation of the control of an X4-flyer shows the good performance of the proposed control algorithm.

References

- [1] E. Altug, J. Ostrowski, and R. Mahony. Control of a quadrotor helicopter using visual feedback. In *Proceedings of the IEEE International Conference on Robotics and Automation, ICRA2002*, Washington DC, Virginia, USA, 2002.
- [2] B. Espiau, F. Chaumette, and P. Rives. A new approach to visual servoing in robotics. *IEEE Transactions on Robotics and Automation*, 8(3):313–326, 1992.
- [3] M. Dahlen E. Frazzoli and E. Feron. Trajectory tracking control design for autonomous helicopters using a backstepping algorithm. In *Proceedings of the American Control Conference ACC*, pages 4102–4107, Chicago, Illinois, USA, 2000.
- [4] E. Frazzoli, M. A. Dahleh, and E. Feron. Real-time motion planning for agile autonomous vehicles. *AIAA Journal of Guidance, Control, and Dynamics*, 5(1):116–129, 2002.
- [5] T. Hamel, R. Mahony, R. Lozano, and J. Ostrowski. Dynamic modelling and configuration stabilization for an X4-flyer. In *International Federation of Automatic Control Symposium, IFAC 2002*, Barcelona, Spain, 2002.
- [6] T. Hamel and R. Mahony. Visual servoing of an under-actuated dynamic rigid-body system: An image based approach. *IEEE Transactions on Robotics and Automation*, 18(2):187–198, April 2002.
- [7] S. Hutchinson, G. Hager, and P. Cork. A tutorial on visual servo control. *IEEE Transactions on Robotics and Automation*, 12(5):651–670, 1996.
- [8] M. Krstic, I. Kanellakopoulos, and P. V. Kokotovic. *Nonlinear and adaptive control design*. American Mathematical Society, Rhode Islande, USA, 1995.
- [9] R. Mahony and T. Hamel. Robust trajectory tracking for a scale model autonomous helicopter. *To appear in the International Journal of Non-linear and Robust Control*, 2003.
- [10] E. Malis and F. Chaumette. Theoretical improvements in the stability analysis of a new class of model-free visual servoing methods. *IEEE Transaction on Robotics and Automation*, 18(2):176–186, 2002.
- [11] Y. Ma, J. Kosecka, and S. Sastry. Vision guided navigation for a nonholonomic mobile robot. *IEEE Transactions on Robotics and Automation*, 15(3):521–536, 1999.
- [12] C. Samson, M. Le Borgne, and B. Espiau. *Robot Control: The task function approach*. The Oxford Engineering Science Series. Oxford University Press, Oxford, U.K., 1991.
- [13] O. Shakernia, Y. Ma, T. J. Koo, and S. Sastry. Landing an unmanned air vehicle: vision based motion estimation and nonlinear control. *Asian Journal of Control*, 1(3):128–146, 1999.